Torres-Carrasco, M., et al. Improvement of thermal efficiency in cement mortars by using synthetic feldspars, In: *Construction and building materials Vol.269, 121279, Feb. 2021, 7 pp.*

DOI: https://doi.org/10.1016/j.conbuildmat.2020.121279

Contents lists available at ScienceDirect

Construction and Building Materials

journal homepage: http://ees.elsevier.com

Improvement of thermal efficiency in cement mortars by using synthetic feldspars

M. Torres-Carrasco [a,b,1,*], E. Enríquez [a,c,1], L. Terrón-Menoyo [a], M.J. Cabrera [c], D. Muñoz [c], J.F. Fernández [a]

[a] Electroceramics Department, Instituto de Cerámica y Vidrio, CSIC, Kelsen 5, 28049 Madrid, Spain
[b] Materials Science and Engineering Department-IAAB, University Carlos III of Madrid, Avda. Universidad 30, 28911 Leganés, Madrid, Spain
[c] Centro Tecnológico Vidres, S.L., Ctra. Onda, Km 3.4, 12540 Villareal, Castellón, Spain

ARTICLE INFO

Article history:
Received 4 July 2020
Received in revised form 6 October 2020
Accepted 7 October 2020
Available online xxx

Keywords
Mortars
Feldspar
Sustainability
Thermal properties

ABSTRACT

The use of white cements as a building material is widely employed due to its high whiteness and reflectance. However, building materials should adopt better thermal insulation characteristics to contribute for a significant urban heat-islands mitigation. In this work, synthetic feldspar has been evaluated as partial and total replacement of sand in white cement mortars. Thermal, mechanical, and optical properties of these new mortars are characterized by thermal conductivity, compression resistance test and reflectance-colorimetry, respectively. The replacement of sand by synthetic feldspar allows to obtain white mortars having ≈18% improvement in solar reflectance. Experiment under solar irradiance of mortars having synthetic feldspars reduce the surface heating of the mortar in 25% and the heating transmission to the rear of the mortar in >55%. Moreover, the high crystallinity of the synthetic feldspar reduces the mortar expansion due alkali-silica reactions (ASR). Improvement in reflectance and thermal conductivity resistance of white cement mortar having synthetic feldspar opens a wide range of building material applications.

1. Introduction

Heat-island is an effect that has been gaining relevance nowadays. The effect is produced by heat accumulation in urban areas by the absorbent materials of which the buildings are made. Heat-island is an evident phenomenon in large cities where buildings and roads do not allow enough heat dissipation during night hours [1–6]. The agglomeration of population, especially in urban areas, alter the energy balance, modifying the pattern of ventilation and causing an increase in radiation.

To the above, it is added that the construction materials do not change their thermal properties, producing a constant energy storage. It is, therefore, essential that the architectural designs incorporate buildings with green spaces that propitiate the conservation of humidity levels in large cities [2,4,5]. It is also imperative to apply a type of construction with new materials that reduce solar radiation (high albedo) [7–9] and that the design favors the ventilation of interior spaces, the use of mass transport systems with clean energy and the promotion of the creation of natural spaces in cities [1,10–15].

With regard to the use of new building materials that favor a considerable saving of energy, it is worth to highlight the use of white based Portland cements with superior decorative properties for cladding of facades and interior [16–18]. White cement has a whiteness greater than 85% compared to a gray cement [19]. To obtain white Portland cements a lower amount of transition metals cations, mainly manganese and iron oxides, must be used in the chemical composition than in a conventional Portland cement. The white color is due to the chemical reactions during clinkering without the presence of chromophore cations as iron oxides and the further grinding with gypsum [19].

One of the main materials that are used as façade coverings are mortars made with white cement and sand [18]. The white mortars give a final decorative appearance and reduce the temperature at the façades surface and, therefore, the heat transmission to the building interior. Thus, white mortar coating favors a reduction in building energy costs by decreasing need for air conditioning in summer time. As consequence, white mortars have a positive impact in reduction of emissions from the use of fossil fuels (CO_2, SO_x, NO_x, etc) [20]. It is estimated that an area of 100 m^2 covered with a white mortar material compensates the emissions of 10 tons of CO_2 throughout its useful life [21]. However, when using coating mortars, the whiteness is affected if conventional sand is used as aggregate, which usually has a reddish hue due to the iron oxide impurities. That is why it requires the use of other alternative materials that make the function of aggregate and that, in addition, increase as much as possible their whiteness. In addition, the search for other alternative materials to Portland cement or that partially replace it is interesting from the point of view of the circular

* Corresponding author at: aElectroceramics Department, Instituto de Cerámica y Vidrio, CSIC, Kelsen 5, 28049 Madrid, Spain.
E-mail address: mtorres@icv.csic.es (M. Torres-Carrasco)
[1] These authors contributed equally to this work.

https://doi.org/10.1016/j.conbuildmat.2020.121279
0950-0618/

economy and the new strategies that Europe is adopting to minimize the problem of the greenhouse effect.

On the other hand, feldspars are natural materials with interesting mechanical and thermal properties. They are the most abundant minerals in nature. However, the use of feldspar in cementitious applications is limited due their alkali content, which could favor the alkali-silica reactions (ASR) degrading the mortar due to the expansion phenomena. This effect is a very important problem that involves great amount of research works, where the alkalis release in pore solution and the mortar expansion is studied by the influence of several parameters, such as humidity, pH, temperature, etc [22–24]. At present, new synthetic feldspar is developed in order to be able to design and develop new functional properties. In previous works, a new glass–ceramic feldspar based on anorthite phase ($CaSi_2Al_2O_8$) was designed [3]. This synthetic feldspar possesses high crystallinity, >92%, and a unique microstructure consisting on anorthite nano and microcrystals. This nano-microstrucure provides large amount of grain boundaries that modifies the thermal, optical and electrical properties of these synthetic feldspars. The use of synthetic feldspar in ceramic provides high solar reflectivity and low thermal diffusivity, allowing an improvement in the energy saving of the buildings, up to 22%, when it is used in linings both outside and inside of buildings [3].

Therefore, in this work, a substitution of sand by the synthetic feldspar has been carried out in order to improve the whiteness of mortars and modify their thermal properties. Hence, thermal, mechanical and optical properties of these new mortars are characterized by thermal conductivity, compression resistance test and reflectance-colorimetry, respectively. It is also studied the influence of the alkalis present in feldspar on the expansion effect of the mortar, carrying out ASR tests.

2. Experimental procedure

2.1. Materials

The chemical composition and the physical properties of the different materials used are given in Table 1 and Table 2, respectively. White Portland cement (WPC, 42.5R) was used in this study. The average particle size was 11.04 μm and the specific surface (BET) was 1.65 m^2/g. In addition, a glass–ceramic material based on anorthite feldspar was used in the mortars preparation as replacement of normalized sand. This material has a short amount of glassy phase, lower than 8%. The similar chemical element composition of white cement and synthetic feldspar, mainly based on Al, Ca and Si, favors the compatibility of the mixture. The synthetic feldspar was ground with a hammer mill to obtain particles having a size between 63 μm and 1 mm, with a similar particle distribution of sand, which has particles between 45 μm and 2 mm, in order to simulate the sand behavior.

2.2. Mortar preparation

Mortar specimens measuring 4 × 4 × 16 cm were prepared with the compositions given in Table 3. Composition with 100 wt% of sand (100S-0F) is used as reference mortar. Composition with substitution of 0, 25, 50, 75 and 100 wt% of sand by feldspar were prepared and named 75S-25F, 50S-50F, 25S-75F and 0S-100F respectively. The liquid/solid ratio (water/cement ratio) was different depending on the samples, searching, in all cases, for the same consistency (values of the diameter of spread of 150 ± 10 mm), as recommended in European standard UNE EN 1015-6. The mortars were cured in a chamber with a 99% relative humidity and at temperature of 22 ± 2 °C for 28 days. The prismatic specimens were tested for mechanical strength at 28 days.

For thermal conductivity and reflectance measurements, mortar specimens measuring 5 cm in diameter by 1 cm thickness (cylindrical) were prepared and, to determine the solar simulation experiments, mortars samples of 14 × 12 × 1 cm were prepared, always following a similar curing procedure than the prismatic specimens.

2.3. Methods

All tests were carried out after 28 days of curing.

The compression resistance test was carried out according to the standard UNE-EN-196-1 in specimens of 4x4x16 cm. The compression test was performed at a uniform speed of 2400 ± 200 N/s until rupture. The equipment used was a hydraulic press of 150 T Ibertest with Servosis automation.

Porosity was measured by means of PoreMaster® mercury intrusion porosimeter (Quantachrome instruments) for high-resolution pore size measurements in the range from 7 nm to 250 μm pore diameter.

ASR tests were carried out by introducing the prepared mortar specimens in an autoclave at 130 °C at 1.7 bar of pressure for 5 h, in order to accelerate the possible alkali-silica reactions that could occur. The sample dimensions were measured before and after 14 days of the trial, according to the ASTM C1778 based on 14-day expansions in ASTM C1260, to obtain their expansion degree [23].

Thermal conductivity measurements of samples were obtained at room temperature by means of DTC-25 Conductivity meter of TA Instrument using the guarded heat flow method.

The colorimetric behavior of the samples was evaluated through the use of the CIE L*a*b* coordinates, the most common uniform color space, using a colorimeter Konica Minolta, Spectra Magic NX, with Color Data Software CM-S100w. L* measures from white to black (0–100), a* measures from green to red and b* from blue to yellow.

The reflectance measurements were carried out by a Perkin Elmer Lambda 950 spectrophotometer with an integration sphere to obtain the total reflectance (diffuse and direct reflectance) in the solar spectrum range (300–2500 nm) with a step of 3 nm.

The solar simulation measurements consist in irradiating the surface sample with the simulator lamp with the aim to obtain the thermal behavior of samples in the entire solar spectrum with the corresponding intensity in each wavelength. Sample surfaces were irradiating up to 3 h. The achieved temperature at the surface was simultaneously measured with a thermal infrared camera and at the same time, temperature transmitted through the sample at the rear part was measured by means a thermocouple placed in the rear side of the mortar specimens.

Table 1
Chemical composition of different materials used (determined by XRF and expressed in terms of wt% equivalent oxides).

Material	wt %									
	CaO	SiO_2	Al_2O_3	MgO	Fe_2O_3	Na_2O	K_2O	TiO_2	P_2O_5	ZrO_2
White cement	65.0	18.6	3.15	0.40	0.14	–	0.27	0.05	–	–
Glass ceramic (feldspar)	11.8	47.9	21.4	0.57	0.23	4.58	1.65	0.11	< 0.01	7.31
Sand	0.10	98.2	0.28	0.03	1.13	0.03	0.01	0.02	–	–

Table 2
Physical properties of the different materials used.

Material	Density (g/cm ^{3})	Thermal conductivity (W/mK)	(*L)	Reflectance (%)	Particle size
White cement	3.08	0.59	87.7	62.8	11.4 μm
Glass ceramic (feldspar)	2.65	0.35	98.1	99.8	63 μm–1 m
Sand	1.60	1.60	54.2	51.9	45 μm–2 m

The data obtained by the thermocouple and the thermocamera were processed by a homemade and commercial software, respectively. Therefore, it is possible to obtain heating curves in both sides of the sample with rather high resolution, which gives information about the reflective capacity and the in situ heat transfer through the sample, related with the thermal diffusivity [3]. The solar simulation experiments were performed by a LCS-100 solar simulator (Lasing S.A.) with a Xenon lamp of 100 W. The simulator possesses an AM1.5G filter (applied to the Standard G-173-03 with 1.5 air mass) that reproduces the solar spectrum with one sun equivalent power which allows measuring the reflective effect of the solar radiation on the samples. The solar filter is 81011-LCS with 2″ square AM0 filter mounted in frame. In addition, the solar simulation includes an AM1,5G spectral correction filter which shapes the light output to closely match the total (direct and diffuse) solar spectrum on the Earth's surface, at a zenith angle of 48.23 (ASTM 892). This provides a Class A irradiance spectrum suitable for photovoltaic testing. The thermal properties were measured by means of a thermal infrared camera FLIR E30 with an image resolution of 160 × 120 pixels and a temperature range of −20 to 350 °C with 0.1 °C of thermal resolution; and with a PT100 thermocouple connected to a multimeter Keithley 2410–1100 V, in voltage and current ranges of 0–100 V and 0–21 mA, respectively. The thermocouple system was calibrated using the cold focus method.

3. Results and discussion

3.1. Mechanical strengths, porosity and ARS test

Fig. 1 shows the results obtained by compression test for each composition. The sample with the best mechanical behavior was the reference mortar sample (100S-0F). As the synthetic feldspar replaces the sand, a loss of compression strength occurs. When the aggregate substitution was 100%, a compression resistance decay to approximately 35% of the value corresponding to the reference mortar. The smaller particle size of the synthetic feldspar demands greater liquid amount, as seen in Table 3, which resulted in a porosity increase that clearly affects the mechanical resistance, as seen in Fig. 1. As the mortars are not designed for structural applications, their compression value required should be >17.2 MPa, according with ASTM C 270, M type mortar intended for exterior applications. So, the value of compression strength achieved by the total replacement of sand by feldspar is still higher than the required for such application. In the case of porosity, the volume of pores increases in more than double, which affects, as explained, in the mechanical properties. Furthermore, the fact that properties are affected causes the behavior of some functional properties to be positive, as will be seen below.

From the mechanical results obtained, it was decided to focus the functional analysis only in the selected mortars, especially in compositions 100S-0F, 75S-25F and 0S-100F.

In a previous work, a study of the reaction of the synthetic feldspar with cement was carried out, obtaining that few amount of feldspar reacted with cement, and the other part remained unreacted transferring its properties to the composite [25]. In this case, the particle size of synthetic feldspar is quite larger than in the previous work, (64 μm–1 mm versus 12 μm), so it is expected that it is less reactive with ce-

Table 3
Mortar dosage of cement having different percentages of sand/feldspar.

Sample	Cement (g)	Water (g)	Sand (g)	Feldspar (g)	% of aggregates (sand/feldspar)	L/S	Consistency (mm)
100S-0F	450.0	225.0	1350.0	0	100/0	0.50	151.0
75S-25F	450.0	247.5	1012.5	337.5	75/25	0.55	151.5
50S-50F	450.0	292.5	675.0	675.0	50/50	0.65	152.5
25S-75F	450.0	337.5	337.5	1012.5	25/75	0.75	152.8
0S-100F	450.0	360.0	0.0	1350.0	0/100	0.80	153.0

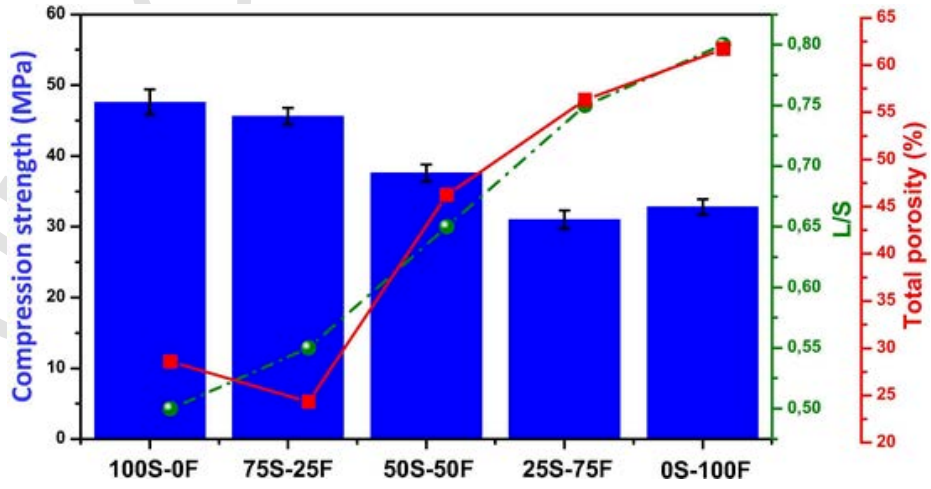

Fig. 1. Compression strength (bars), total porosity (squares) and L/S ratio (circles) of the different systems evaluated after 28 days of curing.

ment, transferring all its properties to mortar. In the XRD patterns presented in the Figure S1 of supporting information it can be confirmed that the mortar with the 100% of feldspar possesses mainly crystalline feldspar and cement phases without presence of quartz phase. This fact corroborates that most of the feldspar remains unreacted and no additional phases are formed.

The ASR was evaluated by the expansion test and the results are presented in Table 4.

According to the ASTM C1260, mortar expansions after 14 days are categorized as: $<0.15\%$ means non-reactive (NR) aggregates, variations $\geq 0.15\%$ suggest moderate reactive (MR) aggregates, and finally, variations $>0.25\%$ determinate high reactive (HR) aggregates. Therefore, regarding the results observed in Table 4, it can be concluded that reference mortar possesses moderate reactive aggregates (sand), experiencing an expansion of 0.15%. However, when sand is substituted by the synthetic feldspar the reactivity of the aggregates is reduced, especially for the complete substitution of sand, where the expansion is as low as 0.01%. This reduction in the expansion effect for mortars using only synthetic feldspar with the white cement can be attributed to a reduced silica content in feldspar (47.9 wt%) regarding to the sand. In addition, in a previous works [25], the alkalis released in pore solution of cement pastes, when cement was substituted by this synthetic feldspar suggest that the alkalis lixiviation is not significant. Therefore, it can be concluded that replacing of sand by synthetic feldspar produces a significant reduction in expansion due to its lower silica content, which reduces the ASR.

Table 4
Mortar expansion measures obtained in the ASR tests after 14 days.

Sample	ΔL (mm)	ΔL/Lx100	Classification
100S-0F	0.18	0.15	MR
75S-25F	0.13	0.11	NR
0S-100F	0.01	0.01	NR

Table 5
Values of L*, a* and b* of cement mortars at 28 days with different percentages of feldspar.

Sample	L*	a*	b*
100S-0F	91.05	−0.15	2.1
75S-25F	91.65	−0.21	1.67
0S-100F	93.31	−0.18	0.42

3.2. Optical measurements

The CIEL*a*b coordinates were measured for all systems evaluated to extract information about the new materials. The results can be seen in Table 5. One of the main objectives of this work is to provide new construction materials intended for the cladding of facades which, in addition, provide higher whiteness. The white cement mortars made with standardized sand have values of a*, b* and L* far from the ideal conditions (0, 0, 100, respectively). This is mainly due to the fact that the incorporated sand has a composition with certain amount of iron oxides (Table 1) that produce a slight yellow coloration, that is, the b* coordinate is 2.1 (see Table 5). However, as the sand is replaced by the synthetic feldspar in different proportions (75S-25F and 0S-100F) a considerable change in the values is observed, especially regarding lightness (L*) and the b* coordinate. When the totality of sand is replaced by feldspar, an improvement of the b* value is reached. In addition, incorporating synthetic feldspar (see Table 2) also provides an increase of the lightness.

In addition, complementary to the study of the CIEL*a*b coordinates, the reflectance measurement provides more information about their ability to reflect sunlight in UV, visible and the infrared (UV–Vis-NIR) regions. Fig. 2a shows the reflectance curves for the three evaluated mortars. As sand has been replaced by feldspar, it is observed higher reflectance than the reference mortar at the age of 28 days. Moreover, this difference is quite important in the NIR range due mainly to the fact that the synthetic feldspar has a greater reflection in the NIR [3].

Fig. 2b shows the solar reflectivity of these three samples, which is obtained from the reflectance spectra, and gives the proportion of the solar radiation reflected back to the atmosphere by the studied material surface, following the Standard Test Method for Solar Absorptance, Reflectance, and Transmittance of Materials Using Integrating Spheres (ASTM E903-96). This concept can be expressed with the solar reflectance (SR) [26,27] which is calculated with the formula of equation (1) in the whole solar spectrum (300–2500 nm).

$$SR = \frac{\int_{300}^{2500} RI_{\lambda} d\lambda}{\int_{300}^{2500} I_{\lambda} d\lambda} \quad (1)$$

where R is the measured spectral reflectivity and I_{λ} the spectral irradiance of the sun at the earth surface (W/(m^{2}nm)), according to the

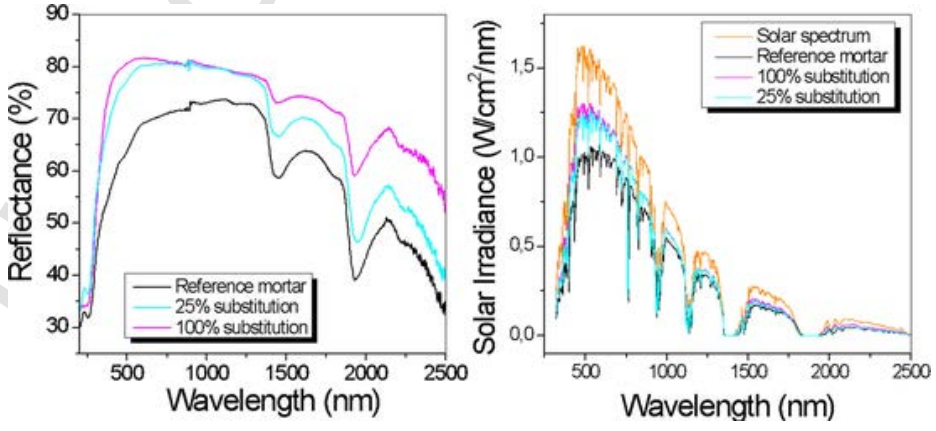

Fig. 2. a) Reflectance curves and **b)** spectral reflectivity compared to the solar spectrum of the systems evaluated with different percentages of sand replacement by feldspar (25% and 100%) after 28 days of curing.

ASTM Standard G-173-03 which is the most commonly standard used for edification applications [20,28].

SR value goes from 0 to 1, where 0 indicates the maximum solar energy absorption and 1 corresponds to the total solar energy reflectance. Therefore, the higher the solar reflectance, the closer the curve to the solar spectrum looks, being the maximum when both spectra coincide. As seen in Fig. 2b, mortars with synthetic feldspar highly reflect the solar spectrum, resembling to it, in comparison to the reference mortar, both in the visible and in the NIR range. Table 6 shows the average reflectance values and solar reflectivity (SR) of the three studied mortars. As seen, the reflectance is increased up to 13% when sand is completely substituted by synthetic feldspar. The solar reflectance is also increased in 12% with synthetic feldspar substitution, indicating a reduction of the material's heating and, therefore, a reduction of heat islands when these materials are used in buildings.

3.3. Thermal properties

Thermal conductivity of the selected compositions was measured since this parameter stablishes the capacity of the material to transfer heat, which is an interesting variable to study for building materials. Thermal conductivity is strongly influenced by density, structure and heat capacity of the sample. The values of the thermal conductivity decrease also with the substitution of sand by feldspar (see Table 7). Thermal conductivity measured for reference mortar is similar to the tabulated values (0.70–0.86) [11,29]. This value is quite low compared to other building materials such as ceramic tiles or reinforced concrete, due to the high porosity of mortars. However, when sand is substituted by a more insulating material, as the synthetic feldspar, thermal conductivity is reduced to values close than wood, which is the building material with best thermal comfort since it has thermal conductivity similar to skin [30,31]. The thermal conductivity reduction is in part due to the increase of porosity for larger L/S ratio and in part for the lower thermal conductivity of synthetic feldspar. Therefore, as seen in Table 7, when 25 wt% of sand is substituted for feldspar, the thermal conductivity is reduced to 0.64 W/mK, and when the substitution is complete (100 wt% feldspar), the value achieves 0.35 W/mK. As seen in Fig. 1, porosity is duplicated when the 100% of sand is substituted by the synthetic feldspar. This increase could suppose a reduction of the thermal conductivity to half the value of the reference mortar. However, the reduction is greater, so the thermal insulating properties of feldspar favor the decrease in thermal conductivity. Hence, these new mortars, being more insulating and, therefore, good candidates to be used as sustainable building material.

Table 6
Average reflectance and solar reflectivity values for the chosen materials.

Sample	Average reflectance (%)	SR
100S-0F	58.82	0.67
75S-25F	66.47	0.77
0S-100F	71.53	0.79

Table 7
Thermal conductivity values for the different prepared mortars at 28 days.

Sample	Thermal conductivity (W/mK)
100S-0F	0.86
75S-25F	0.64
0S-100F	0.35

Fig. 3 shows the measurements obtained for the solar simulation experiment on selected mortars (Fig. 3a). Measurements are expressed in temperature gradients in order to normalize with the room temperature. Thick lines represent the temperature gradient in the sample surface, taken with the infrared thermocamera and the thin lines represent the temperature gradient at the mortar back obtained with the thermocouple, when the solar simulator irradiates the sample up to 180 min. For shake of clarity, the measurements up to 300 s are also included to provide information about the dynamic regime of heating that shows large variation of temperature. Hence, higher reflectance would produce lower heating at the surface and lower heat propagation to the mortar rear due a lower thermal diffusivity of the mortar. In all cases, the reference mortar presents larger temperature gradient, both in the surface and in the rear part, than mortars with synthetic feldspar. This fact indicates lower reflectance, as seen in previous section, and larger heat propagation through the sample. Mortar with larger percentage of synthetic feldspar presents large reduction of heating at the surface, compare with the reference mortar in the dynamic regime (1.2 °C lower up to 300 s) and in the stationary regime (6 °C after 180 min).

However, the difference of heating between the rear parts is quite larger (1 °C lower in case of 100 wt% feldspar composition), indicating that the high feldspar content avoids the heat propagation through the sample. Fig. 3c, d and e show the thermograph images extracted from the thermocamera after 5 min of solar irradiation, showing the difference in the surface heating. If the heating experiment is prolonged by maintaining the illumination for 3 h, it is possible to check that a stationary temperature is reached, and the heating rate is maintained, being the reference mortar the most heated and the 100% substituted the

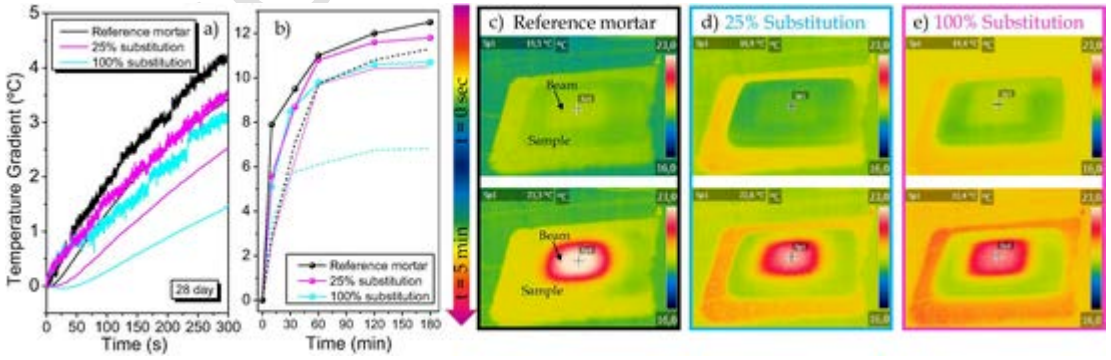

Fig. 3. a) Heating curves obtained by the solar simulation experiment for mortars at 28 days. The thick lines represent the temperature gradient in the samples surface and the thin lines represent the temperature gradient of the rear part, when the solar simulator irradiates the sample during 5 min. b) Heating curves of samples when the simulation experiment is maintained during 3 h. Figures c, d and e shows the thermograph images extracted from the thermal camera after 5 min of solar irradiation for reference, 25 wt% and 100 wt% substitution by synthetic feldspar, respectively.

least one, with almost 2 °C of difference. Moreover, the difference in the rear part heating is also very significant, being the 100% substituted mortar the least heated (Fig. 3b). This fact supposes an advantage for a building material, since it would act as thermal insulating, avoiding the outside temperature propagation to the building interior. This fact represents an improvement in the thermal efficiency of a mortar coating for facades. Reduction in ≈ 1 °C in the building interior could suppose a 20% of energy saving in a building acclimatization [2,3,8].

4. Conclusions

Sand has been successfully substituted in white cement by synthetic glass–ceramic feldspar, in order to improve its whiteness and its thermal and optical properties. The substitution worsens the mortars resistance due to the need of increasing the L/S proportion which produces a porosity increase. However, compression strength is within the standard requirements. The substitution of sand by synthetic feldspar reduces considerably the ASR effects of mortars due to the low alkalis lixiviation, and its lower silica content.

On the other hand, the optical and thermal properties are highly improved. The achieved whiteness of mortars is favorable for the aesthetic application and for solar light reflection (albedo). Moreover, the thermal conductivity is reduced when sand is substituted by feldspar, achieving very low values. This fact provides white mortars with high thermal insulation capacity, since it avoids the heat propagation to the inside of the building and achieves a better maintaining of inside temperature, which can promote energy savings for temperature conditioning. Therefore, these new mortars with improved properties would provide a new chance for more sustainable building materials with superior aesthetic properties. These materials are good candidates to be used in façades to reduce heat-islands in cities.

CRediT authorship contribution statement

M. Torres-Carrasco: Conceptualization, Methodology, Formal analysis, Investigation, Resources, Data curation, Writing - review & editing, Visualization. **E. Enríquez:** Conceptualization, Methodology, Formal analysis, Investigation, Resources, Data curation, Writing - review & editing, Visualization. **L. Terrón-Menoyo:** Investigation, Methodology, Resources, Writing - review & editing, Supervision. **M.J. Cabrera:** Conceptualization, Funding acquisition, Methodology, Resources, Writing - review & editing, Supervision. **D. Muñoz:** Conceptualization, Funding acquisition, Methodology, Resources, Writing - review & editing, Supervision. **J.F. Fernández:** Conceptualization, Formal analysis, Funding acquisition, Investigation, Methodology, Resources, Writing - original draft, Supervision.

Declaration of Competing Interest

The authors declare that they have no known competing financial interests or personal relationships that could have appeared to influence the work reported in this paper.

Acknowledgements

The authors express their thanks to the Project MAT-2017-86450-C4-1-R, CSIC NANOMIND project CSIC2015-60E068 and projects CDTI (IDI-20130894 and IDI-20161120) for their financial support. Dra. E. Enríquez is indebted to MINECO for a ''Torres Quevedo'' contract (ref: PTQ-14-07289), which is co-financed with European Social Funds. Dr. M. Torres-Carrasco is also indebted to MINECO for a postdoctoral fellowship "Juan de la Cierva-Formación" (ref: FJCI-2016-28488).

Appendix A. Supplementary data

Supplementary data to this article can be found online at https://doi.org/10.1016/j.conbuildmat.2020.121279.

References:

[1] E.S. Cozza, M. Alloisio, A. Comite, G. Di Tanna, S. Vicini, NIR-reflecting properties of new paints for energy-efficient buildings, Sol. Energy. 116 (2015) 108–116, doi:10.1016/j.solener.2015.04.004.
[2] M.H. Chung, J.C. Park, M.J. Ko, Effect of the solar radiative properties of existing building roof materials on the energy use in humid continental climates, Energy Build. 102 (2015) 172–180, doi:10.1016/j.enbuild.2015.05.022.
[3] E. Enríquez, V. Fuertes, M.J. Cabrera, J. Seores, D. Muñoz, J.F. Fernández, New strategy to mitigate urban heat island effect: energy saving by combining high albedo and low thermal diffusivity in glass ceramic materials, Sol. Energy. 149 (2017), doi:10.1016/j.solener.2017.04.011.
[4] M. Santamouris, Cooling the cities – a review of reflective and green roof mitigation technologies to fight heat island and improve comfort in urban environments, Sol. Energy. 103 (2014) 682–703, doi:10.1016/j.solener.2012.07.003.
[5] A.L. Pisello, Experimental analysis of cool traditional solar shading systems for residential buildings, Energies. 8 (2015) 2197–2210, doi:10.3390/en8032197.
[6] S. Kinoshita, A. Yoshida, Investigating performance prediction and optimization of spectral solar reflectance of cool painted layers, Energy Build. 114 (2016) 214–220, doi:10.1016/j.enbuild.2015.06.072.
[7] R.M. Akbahi, H., Behre, A., Levinson, R., Graveline, S., Foley, K., Delgado, A.H., and Paroli, H. Akbari, A.A. Berhe, R. Levinson, S. Graveline, K. Foley, A.H. Delgado, R.M. Paroli, R.M. Akbahi, H., Behre, A., Levinson, R., Graveline, S., Foley, K., Delgado, A.H., and Paroli, Aging and weathering of cool roofing membranes, Cool Roof. Symp. Atlanta, GA. (2005) 1–11, doi: 10.1017/CBO9781107415324.004.
[8] T. Ihara, A. Gustavsen, B.P. Jelle, Effect of facade components on energy efficiency in office buildings, Appl. Energy. 158 (2015) 422–432, doi:10.1016/j.apenergy.2015.08.074.
[9] C.M. Álvarez-Docio, J.J. Reinosa, A. del Campo, J.F. Fernández, 2D particles forming a nanostructured shell: a step forward cool NIR reflectivity for $CoAl_2O_4$ pigments, Dye. Pigment. 137 (2017) 1–11, doi:10.1016/j.dyepig.2016.09.061.
[10] L. Wang, Y. Dong, S.H. Zhou, E. Chen, S.W. Tang, Energy saving benefit, mechanical performance, volume stabilities, hydration properties and products of low heat cement-based materials, Energy Build. 170 (2018) 157–169, doi:10.1016/j.enbuild.2018.04.015.
[11] J. Li, W. Chen, Heat transfer dynamic analyses for recycled-concrete wall combined with expanded polystyrene template, Adv. Mater. Sci. Eng. 2018 (2018), doi:10.1155/2018/9692806.
[12] E.S. Bakhoum, G.L. Garas, M.E. Allam, H. Ezz, The role of nano-technology in sustainable construction: a case study of using nano granite waste particles in cement mortar, Eng. J. 21 (2017) 217–227, doi:10.4186/ej.2017.21.4.217.
[13] A. Antonaia, F. Ascione, A. Castaldo, A. D'Angelo, R.F. De Masi, M. Ferrara, G.P. Vanoli, G. Vitiello, Cool materials for reducing summer energy consumptions in Mediterranean climate: in-lab experiments and numerical analysis of a new coating based on acrylic paint, Appl. Therm. Eng. 102 (2016) 91–107, doi:10.1016/j.applthermaleng.2016.03.111.
[14] T. Karlessi, M. Santamouris, K. Apostolakis, A. Synnefa, I. Livada, Development and testing of thermochromic coatings for buildings and urban structures, Sol. Energy. 83 (2009) 538–551, doi:10.1016/j.solener.2008.10.005.
[15] R. Levinson, P. Berdahl, A. Asefaw Berhe, H. Akbari, Effects of soiling and cleaning on the reflectance and solar heat gain of a light-colored roofing membrane, Atmos. Environ. 39 (2005) 7807–7824, doi:10.1016/j.atmosenv.2005.08.037.
[16] Y.H. Chang, P.H. Huang, B.Y. Wu, S.W. Chang, A study on the color change benefits of sustainable green building materials, Constr. Build. Mater. 83 (2015) 1–6, doi:10.1016/j.conbuildmat.2015.02.065.
[17] Y. Ma, Y. Li, B. Zhu, Analysis of the thermal properties of air-conditioning-type building materials, Sol. Energy. 86 (2012) 2967–2974, doi:10.1016/j.solener.2012.07.001.
[18] G. Perez, V.R. Allegro, M. Corroto, A. Pons, A. Guerrero, Smart reversible thermochromic mortar for improvement of energy efficiency in buildings, Constr. Build. Mater. 186 (2018) 884–891, doi:10.1016/j.conbuildmat.2018.07.246.
[19] A.P. Kirchheim, V. Rheinheimer, D.C.C. Dal Molin, Comparative study of white and ordinary concretes with respect of carbonation and water absorption, Constr. Build. Mater. 84 (2015) 320–330, doi:10.1016/j.conbuildmat.2015.03.020.
[20] C. Ferrari, A. Libbra, A. Muscio, C. Siligardi, Design of ceramic tiles with high solar reflectance through the development of a functional engobe, Ceram. Int. 39 (2013) 9583–9590, doi:10.1016/j.ceramint.2013.05.077.
[21] S.H. Cho, C.U. Chae, A study on life cycle CO2emissions of low-carbon building in South Korea, Sustain. 8 (2016) 1–19, doi:10.3390/su8060579.
[22] J. Feiteira, J. Custódio, M.S.S. Ribeiro, Review and discussion of polymer action on alkali-silica reaction, Mater. Struct. Constr. 46 (2013) 1415–1427, doi:10.1617/s11527-012-9983-2.
[23] S.G. Wood, E.R. Giannini, M.A. Ramsey, R.D. Moser, Autoclave test parameters for determining alkali-silica reactivity of concrete aggregates, Constr. Build. Mater. 168 (2018) 683–691, doi:10.1016/j.conbuildmat.2018.02.114.

[24] Z. Owsiak, J. Zapała-Sławeta, P. Czapik, Diagnosis of concrete structures distress due to alkali-aggregate reaction, Bull. Polish Acad. Sci. Tech. Sci. 63 (2015) 23–29, doi:10.1515/bpasts-2015-0003.
[25] E. Enríquez, M. Torres-Carrasco, M.J. Cabrera, D. Muñoz, J.F. Fernández, Towards More Sustainable Building Based on modified Portland Cements Through Partial Substitution by Engineered Feldspars, Constr. Build. Mater. (accepted).
[26] R. Levinson, H. Akbari, P. Berdahl, Measuring solar reflectance-Part I: defining a metric that accurately predicts solar heat gain, Sol. Energy. 84 (2010) 1717–1744, doi:10.1016/j.solener.2010.04.018.
[27] R. Levinson, H. Akbari, P. Berdahl, Measuring solar reflectance-Part II: review of practical methods, Sol. Energy. 84 (2010) 1745–1759, doi:10.1016/j.solener.2010.04.017.
[28] A. Libbra, L. Tarozzi, A. Muscio, M.A. Corticelli, Spectral response data for development of cool coloured tile coverings, Opt. Laser Technol. 43 (2011) 394–400, doi:10.1016/j.optlastec.2009.07.001.
[29] S. Mounir, K. Abdelhamid, Y. Maaloufa, Thermal inertia for composite materials white cement-cork, cement mortar-cork, and plaster-cork, Energy Procedia. 74 (2015) 991–999, doi:10.1016/j.egypro.2015.07.830.
[30] D. Lai, X. Zhou, Q. Chen, Measurements and predictions of the skin temperature of human subjects on outdoor environment, Energy Build. 151 (2017) 476–486, doi:10.1016/j.enbuild.2017.07.009.
[31] M.L. Cohen, Measurement of the thermal properties of human skin. A review, J. Invest. Dermatol. 69 (1977) 333–338.